



HAL
open science

Radial gradient refractive index (GRIN) infrared lens based on spatially resolved crystallization of chalcogenide glass

Enora Lavanant, Laurent Calvez, François Cheviré, Mathieu Roze, Thomas Hingant, Raphael Proux, Yann Guimond, Xiang-Hua Zhang

► To cite this version:

Enora Lavanant, Laurent Calvez, François Cheviré, Mathieu Roze, Thomas Hingant, et al.. Radial gradient refractive index (GRIN) infrared lens based on spatially resolved crystallization of chalcogenide glass. *Optical Materials Express*, 2020, 10 (4), pp.860-867. 10.1364/OME.383868. hal-02562370

HAL Id: hal-02562370

<https://univ-rennes.hal.science/hal-02562370>

Submitted on 12 May 2020

HAL is a multi-disciplinary open access archive for the deposit and dissemination of scientific research documents, whether they are published or not. The documents may come from teaching and research institutions in France or abroad, or from public or private research centers.

L'archive ouverte pluridisciplinaire **HAL**, est destinée au dépôt et à la diffusion de documents scientifiques de niveau recherche, publiés ou non, émanant des établissements d'enseignement et de recherche français ou étrangers, des laboratoires publics ou privés.

Radial Gradient Refractive Index (GRIN) infrared lens based on spatially resolved crystallization of chalcogenide glass

ENORA LAVANANT^{1,2}, LAURENT CALVEZ^{1*}, FRANÇOIS CHEVIRÉ¹, MATHIEU ROZÉ², THOMAS HINGANT², RAPHAËL PROUX², YANN GUIMOND², XIANG-HUA ZHANG¹

¹Univ Rennes, CNRS, ISCR (Institut des Sciences Chimiques de Rennes) - UMR 6226, F-35000 Rennes, France

²Umicore I.R Glass, Z.A du Boulais, 35690, Acigné, France

*laurent.calvez@univ-rennes1.fr

Abstract: While widely used in the visible, radial gradient refractive index (GRIN) lenses are still elusive in the IR waveband. In this paper we introduce a new method based on spatially resolved crystallization of chalcogenide glass to produce such lenses. Optical and structural properties of 80 GeSe₂-20 Ga₂Se₃ glass ceramic samples are measured. A shift of refractive index is induced by increasing the density of nanocrystals. By placing the sample into a tailored thermal profile, spatially controlled crystallization is achieved. To our knowledge this constitutes the first fabrication of an optically functional radial GRIN in the IR. We also introduce a method to characterize the index profile non-destructively, which is a necessary step for embedding GRIN into commercial systems.

1. Introduction

Gradient Refractive Index (GRIN) lenses are optics where the refractive index varies spatially.^[1] Using inhomogeneous index gives more degrees of freedom for the optical design. For example, the use of a specific index profile allows to correct efficiently thermal and chromatic aberrations with a significantly reduced number of lenses compared to a conventional system.^[2, 3] Such attractive prospects explain why GRIN materials are widely used in the visible. Many techniques have been employed for fabrication of GRIN in oxide glasses among which neutron irradiation,^[4] chemical vapor deposition (CVD),^[5] thermal poling,^[6] sol-gel method^[7] and ionic exchange.^[8-11]

Thermal IR optics is a rapidly growing field, with the emergence of low cost and high quality uncooled detectors as well as the increasing availability of various chalcogenide glasses.^[12,13] However, producing GRINs in IR optical materials remains highly challenging despite years of efforts.^[14] Fabricating GRINs in chalcogenide glasses has been achieved by stacking thin layers of glass with distinct refractive indices,^[15-18] by using thermal poling of glass containing mobile ions,^[19] by electrospray printing^[20] and by controlled crystallization^[21, 22] or vitrification^[23] induced by laser. Among these techniques, only layer-stacking and controlled crystallization have been demonstrated on large sizes required to produce lenses. However, the samples produced by stacking or controlled crystallization were axial GRINs, while radial GRINs are more desirable for optical design.^[3]

In this paper, we demonstrate the first fabrication of a radial GRIN for the IR using 80 GeSe₂ – 20 Ga₂Se₃ glass composition, by spatially resolved crystallization.

2. Results and discussion

Chalcogenide glass-ceramics have been widely studied for the improvement of their thermo-mechanical properties.^[24, 25] For this purpose, crystals are generated homogeneously within the glassy matrix. The atomic reorganization of the base glass induces structural changes that lead to a densification of the material. Accompanying this formation of crystallites, a change in the optical properties like the refractive index can be expected. This behavior is already observed for materials as widely used as silicon dioxide (SiO₂) where the index can vary from $n = 1.46$ for amorphous glass to $n = 1.6$ for coesite.^[26] Recently, similar change in optical properties induced by crystallization have also been reported in chalcogenides.^[27-29] With this

respect, a spatially resolved crystallization should lead to a controlled variation of the refractive index within the glass ceramic. This is what we propose to demonstrate in this paper.

With this in mind, we have selected the 80 GeSe₂–20 Ga₂Se₃ base glass as its reproducible crystallization has been extensively studied by Rozé et al.^[30] In order to validate that this material is relevant for a GRIN application, the change in refractive index with the evolution of crystalline structure is characterized by annealing several samples of 80 GeSe₂–20 Ga₂Se₃ base glass at 390 °C in a ventilated furnace for a range of durations up to 72 h. **Figure 1a** shows the evolution of refractive index measured at 1.311 μm and 1.551 μm as a function of annealing time. The refractive index increases from 2.401 at 1.551 μm to a maximum of 2.433 after 32 hours of annealing. It then decreases slowly to 2.422 after 72 hours. **Figure 1b** shows X-ray diffraction patterns of the samples for each annealing time. Each curve is artificially shifted upwards to allow for tracking the evolution of the peaks along time. The diffraction lines expected for crystalline Ga₂Se₃ and GeSe₂ are shown for reference.^[31, 32] This measurement provides information on the crystalline phases present in the sample after different annealing times. The lines associated to Ga₂Se₃ increase gradually from the start and most of them stabilize roughly after 24 h. After 32 hours, GeSe₂ lines start emerging. This behavior is strongly correlated with the evolution of the refractive index which starts decreasing after 32 hours of annealing.

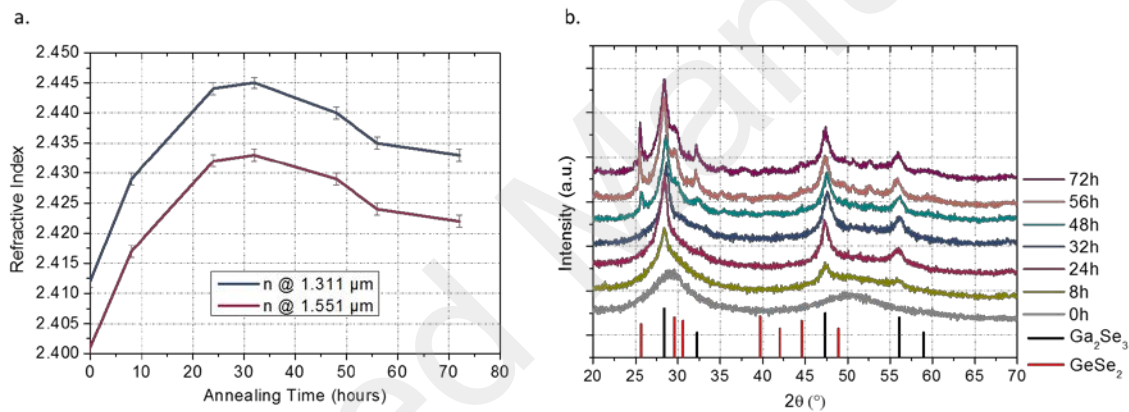


Fig.1. (a) Measured refractive index of 80 GeSe₂–20 Ga₂Se₃ glass and glass-ceramics at 1.311 μm and 1.551 μm and (b) X-ray diffraction patterns of glass-ceramics annealed at 390 °C.

For further understanding, two samples of crystalline Ga₂Se₃ and GeSe₂ were synthesized. The refractive index at 1.551 μm was measured to be 2.579 for Ga₂Se₃ and 2.368 for GeSe₂ when the base 80 GeSe₂ – 20 Ga₂Se₃ glass presents a refractive index of 2.401. The initial increase of refractive index observed on Figure 1a can thus be attributed to the crystallization of Ga₂Se₃ nanoparticles, followed by the germination of GeSe₂ which causes the subsequent decrease of the refractive index.

In addition to enhancing the thermo-mechanical properties of the base glass, the generation of Ga₂Se₃ crystals after 32 hours of annealing induces a large refractive index difference $\Delta n = 3.2 \pm 0.1 \cdot 10^{-2}$ with the base glass. 80 GeSe₂ – 20 Ga₂Se₃ is thus an excellent candidate to produce a GRIN optical element, provided that we dispose of a robust method to control the crystallization spatially.

In the precedent experiment, different crystallization states have been obtained by controlling the annealing time at a constant temperature. However, chalcogenide glasses present the specificity that both nucleation and growth steps partially overlap. Therefore, the crystallization rate can also be controlled by annealing a constant time but at different temperatures. The warmer the annealing, the faster the crystallization. This is the mechanism we propose to use to control spatially the crystallization. The idea is to define a spatially resolved temperature in the material. The crystallization and hence the index should then

mirror the temperature profile. In **Figure 2**, we describe how this process can be used to create a radial GRIN. The base material is a glassy $80 \text{ GeSe}_2 - 20 \text{ Ga}_2\text{Se}_3$ cylinder of 10 mm in diameter and 80 mm in length. During the crystallization process, helium gas flow (of $1.5 \text{ l}\cdot\text{min}^{-1}$) is maintained in order to avoid surface oxidation of the glass. The temperature change in the material is created with an annular furnace at $430 \text{ }^\circ\text{C}$, like illustrated in Figure 2a. The annealing time is controlled by drawing the glass rod at a constant speed of $0.6 \text{ mm}\cdot\text{min}^{-1}$ through the furnace. The drawing together with the low thermal conductivity of the glass prevents the homogenization of temperature inside the rod and produces the desired radial distribution of temperature. Figure 2b illustrates the distribution of temperature inside the rod, which is locally heated at its surface (red) while staying cooler in the center (white). The expected radial distributions of crystallization and refractive index are shown. Heat induces crystallization and is expected to cause an increase of refractive index, similarly to what was observed in Figure 2b.

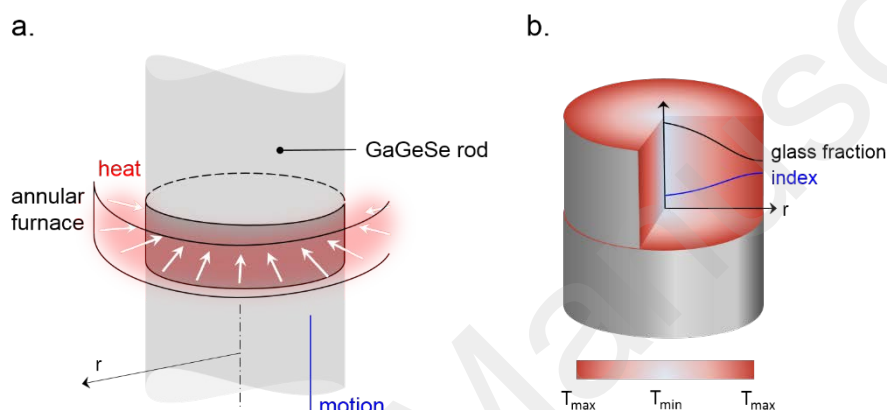


Fig. 2. (a) Schematic diagram of the process and (b) schematic diagram of the creation of the radial GRIN in glasses. The red gradient in figure (b) schematizes the inhomogeneous temperature profile, which should lead to an inhomogeneous radial crystallization.

The rod produced using the method described above is then sliced to characterize the radial distribution of crystallization and refractive index. **Figure 3a** is a picture of such slice, with the positions (d) in the center, (f) at the edge and (e) in between. Figure 3b shows an X-ray diffraction pattern of the center and of the edge of the sample. The broadness of the peaks in the diffractogram measured at the center confirms the glassy nature of the sample which has not had enough time to crystallize. On the edge, the diffractogram displays peaks at $2\theta = 28^\circ$, 47° and 56° that can be indexed by Ga_2Se_3 phase. The lines characteristic to Ga_2Se_3 have been added for reference. One can also note that the lines attributed to the GeSe_2 phase in Figure 1b are not visible in the drawn sample. These two diffractograms support the fact that crystallization happened at the edge of the rod but not in the center, possibly with a continuous distribution along the radius of the rod. This idea is further supported by Figure 3d, e and f which present SEM images of the sample. The sample was cleaved through its center and the images were taken along the cleaved surface from the center to the edge. Figure 3f (at the edge of the sample) shows a high degree of crystallization and a homogenous distribution of Ga_2Se_3 crystals of about 250 nm in size. While moving towards the center of the slice (Figure 3(e) and (d)), the density and size of crystals decrease progressively until having a fully amorphous structure. Finally, Figure 3c presents the transmission spectra taken at positions (d), (e) and (f). These are strongly affected by Fresnel losses of 35 to 50%, which are expected with a refractive index of 2.4. The crystallized phases display a marginally smaller transmission than the center, which can be attributed to additional scattering due to the presence of nanocrystals in the glass. This assumption is further supported by the lower transmission at shorter wavelengths where the scattering is more efficient. Nonetheless, the IR transparency in the third atmospheric window (8-14 μm) remains excellent and compatible

with the use of such a material in an IR optical system. In addition, the progressive crystallization can be expected to cause a distribution of refractive index along the radius of the sample, which would constitute a radial GRIN material.

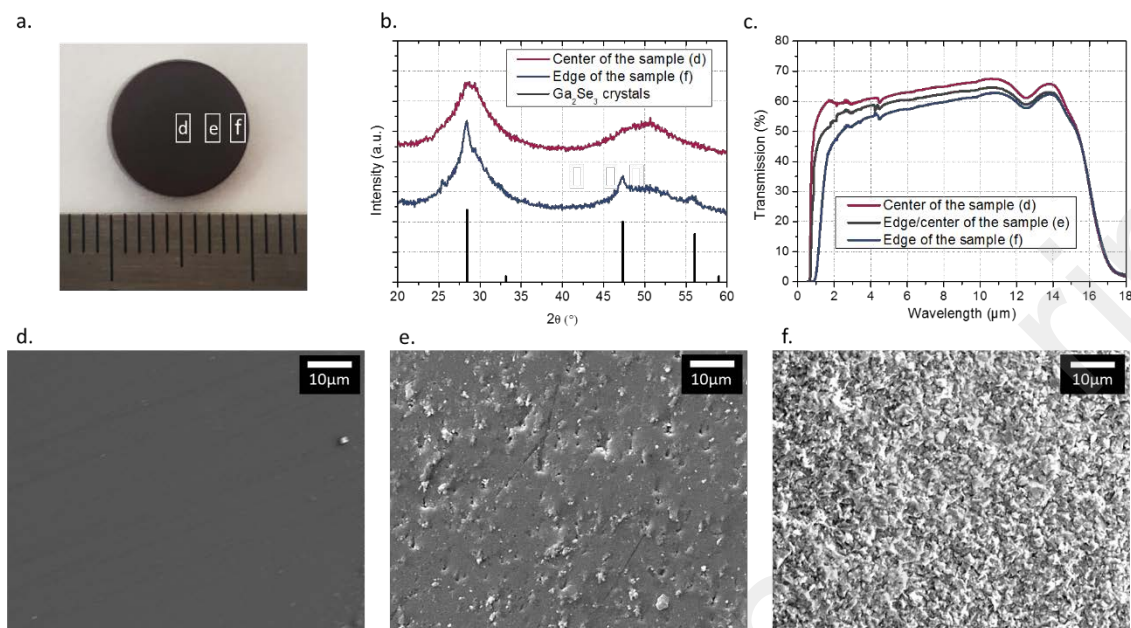


Fig. 3. (a) Image of the glass ceramic after drawing ceramization showing the 3 different places for SEM images. (b) XRD patterns of 80 GeSe₂-20 Ga₂Se₃ glass ceramic at different place after non homogeneous crystallization and Ga₂Se₃ crystals. (c) Effect of the Ga₂Se₃ crystals on infrared transmission at different place in glass ceramic, (d, e, f) SEM images of the 80 GeSe₂-20 Ga₂Se₃ after radial crystallization at different places in the center (d), edge/center (e), and edge of the sample (f).

The first qualitative experiment is described in **Figure 4a**. Disks of the 80 GeSe₂-20 Ga₂Se₃ base glass and of the supposed GRIN material obtained by drawing were polished via Single Point Diamond Turning (SPDT) in order to obtain parallel and flat surfaces (curvature radius $R = 3400$ mm, and roughness $Ra < 7$ nm). In Figure 4b and c, the image of a metallic grid was taken using an infrared camera in the 8-12 μm waveband, respectively through the disk of base glass and through the disk of spatially crystallized material. The image of the metallic grid remains flat and unchanged through the base glass but is compressed at the edge of the crystallized disc. The latter constitutes a signature of the change in refractive index along the radius of the crystallized disc.

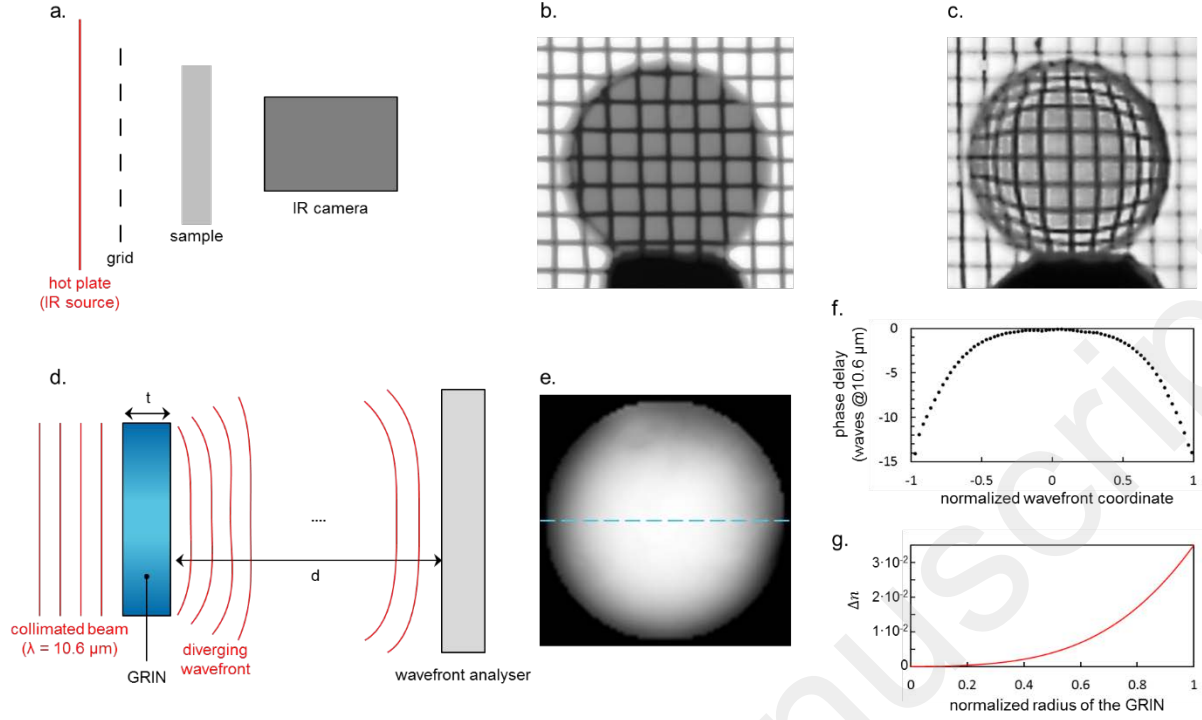


Fig. 4. Optical characterization of the GRIN. (a) Schematic description of the setup used to produce the IR images in (b) with the base glass and in (c) with the partially crystallized material, both of 10 mm diameter and 3mm thick. (d) Description of the interferometric estimation of the index gradient. A collimated beam is propagated through the GRIN parallel plate and the wavefront is recorded by a lateral shear-wave interferometer. (e) Wavefront recorded after propagation through the GRIN. The diameter of the measured wavefront is approximately 10 mm and the maximal difference between black and white corresponds to a 14.01 waves delay. (f) Profile taken along the dashed blue line-cut in image (e). (g) Index gradient inferred from the fit of the profile in (f) with a ray-tracing method.

In order to get a more quantitative characterization of the refractive index gradient, we have attempted to reconstruct the phase delay induced on a collimated CO₂ laser beam at 10.6 μm propagating through the disc. The experiment is schematized in Figure 4d. The wavefront after the propagation has been measured using a quadriwave lateral shearing interferometer developed by Phasics and is reproduced in Figure 4e. Knowing the geometry of the experiment, namely the thickness $t = 3.261 \pm 0.001$ mm of the sample and its distance $d = 12.83 \pm 1$ mm to the interferometer, the propagation through the GRIN has been modelled using the ray-tracing software Optics Studio from Zemax[®].^[33] The radial index profile $n(r) = n_0 + \Delta n(r)$ has been modelled with a sixth order even polynomial function $\Delta n(r) = n_2 r^2 + n_4 r^4 + n_6 r^6$. The value of base index n_0 has been extrapolated from the value at 1.55 μm to be on the order of 2.35 ± 0.02 at a wavelength of 10.6 μm, and the coefficients $n_{2i, i \neq 0}$ have been optimized numerically to best fit the line-cut of Figure 4f, taken across the measured wavefront obtained with the interferometer. The index gradient $\Delta n(r)$ inferred from this fit is plotted in Figure 4g. While this method to assess the gradient remains a crude extrapolation, we have verified that the gradient estimation is insensitive to the uncertainties in the geometry of the experiment and in the base index. From this estimation, the maximal change is $\Delta n_{max} = 3.5 \pm 0.5 \cdot 10^{-2}$, which is of the same order than the maximal change observed in the bulk in our first experiment. This extrapolation therefore gives a good estimation of the refractive index change and could possibly become a quick and non-destructive method to characterize and optimize radial GRINs produced with the method described in this paper. While other techniques such as ellipsometry can achieve non-destructive characterization, interferometry is extremely fast (few seconds) and allows to probe the full volume and homogeneity of the material.

3. Conclusion

This paper reports an innovative way to manufacture radial GRIN infrared lenses based on spatially resolved crystallization. A non-destructive optical method is also proposed to characterize quantitatively the obtained index profile.

The controlled crystallization of Ga_2Se_3 in the $80 \text{ GeSe}_2 - 20 \text{ Ga}_2\text{Se}_3$ generates a progressive shift of the refractive index in the bulk material. After 32 hours of annealing, a maximum refractive index difference of $\Delta n = 3.2 \pm 0.1 \cdot 10^{-2}$ at $1.551 \mu\text{m}$ was measured between the base glass and the glass ceramic. A similar behavior is to be expected when keeping the annealing time and increasing the temperature.

To create a radially resolved crystallization, a radial temperature gradient was generated in the material by displacing it through the center of an annular furnace. The resulting radial crystallization gradient was confirmed by SEM, XRD and transmission measurements, which all describe a material with a high density of crystals on the edge and a glassy structure in the center. The limited size of the crystalline particles limits scattering and the overall transmission remains excellent in both the $3\text{-}5 \mu\text{m}$ and $8\text{-}12 \mu\text{m}$ windows. Our material is thus an ideal candidate for thermal imaging applications.

The crystallization gradient results in a gradient of refractive index. This was verified using a SPDT-polished slice of the treated preform. The image of a metallic grid through the sample appears compressed on the edges which confirms the diverging function of the GRIN. By measuring the wavefront transmitted by the GRIN at $10.6 \mu\text{m}$, the phase delay through the material can be reconstructed and a maximum refractive index difference of $\Delta n_{\text{max}} = 3.5 \pm 0.5 \cdot 10^{-2}$ was assessed, which is in line with bulk measurements.

To our knowledge we report here the very first radial GRIN infrared lens. Spatially resolved crystallization is a very versatile method which is not limited to the $\text{GeSe}_2 - \text{Ga}_2\text{Se}_3$ based composition. With the whole range of chalcogenide glass materials available, it offers an unlimited toolbox for optical design and paves the way towards industrial IR GRIN components.

4. Experimental details

Glass synthesis:

The $80 \text{ GeSe}_2 - 20 \text{ Ga}_2\text{Se}_3$ base glass was synthesized by the vacuum-sealed melt-quenching method.^[12] High purity starting elements of Ge (5N), Se (5N), and Ga (4N), were weighed in stoichiometric proportions and introduced in a 10 mm-diameter silica tube. This tube was evacuated down to 10^{-5} Pa, sealed, and heated up in a rocking furnace for 12 h at $900 \text{ }^\circ\text{C}$ and then lowered to $800 \text{ }^\circ\text{C}$ for 2 hours to avoid thermal convection flows during quenching. The melt was quenched in water at room temperature. The sample was finally annealed at $390 \text{ }^\circ\text{C}$ ($T_g - 20 \text{ }^\circ\text{C}$) for 3 hours to minimize the internal stresses induced by water quenching, before being slowly cooled down to room temperature.

Sample characterization:

DSC measurements were performed on glass samples (10 mg) under nitrogen atmosphere using a heating rate of $10 \text{ }^\circ\text{C}\cdot\text{min}^{-1}$.

The infrared transmission measurements were performed from $2 \mu\text{m}$ to $20 \mu\text{m}$ using a Bruker Vector 22 FTIR Spectrometer. The typical sample thickness was 2 mm after high quality polishing.

X-ray diffraction (XRD) patterns of polished slices were recorded at room temperature in the 2θ range $20^\circ\text{-}80^\circ$ with a step size of 0.052° and a scan time per step of 1200 s using a PANalytical X'Pert Pro diffractometer (Cu K-L_{2,3} radiation, $\lambda = 1.5418 \text{ \AA}$, PIXcel 1D detector). XRD patterns were collected to determine crystalline phases generated during heat treatment.

The refractive index was measured using M-line technique (Metricon 2010/M Prism coupler), at 1.311 μm and 1.551 μm with an accuracy of 1.10^{-3} .

Scanning Electronic Microscope (SEM) coupled with Energy Dispersive Spectroscopy was used to observe crystals within the glass-ceramics from the edge to the center of the bulk after ceramization experiments.

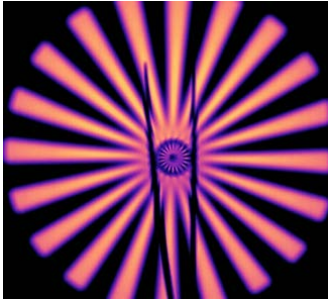
REFERENCES

- [1] D. T. Moore, *Appl. Opt.* **1980**, 19, 1035–1038.
- [2] A. M. Boyd, in Proc. SPIE 10181, **2017**, Adv. Opt. Def. Appl. UV LWIR II, 1018109.
- [3] S. D. Campbell, D. E. Brocker, J. Nagar, & D. H. Werner, *Appl. Opt.* **2016**, 55, 3594–3598.
- [4] P. Sinai, *Appl. Opt.* **1971**, 10, 99–104.
- [5] M. A. Pickering, R. L. Taylor, & D. T. Moore, *Appl. Opt.* **1986**, 25, 3364–3372.
- [6] S. I. Sviridov, & N. P. Eliseeva, *Glass Phys. Chem.* **2006**, 32, 604–611.
- [7] H. Zheng, & Chemat Technology Inc. Northridge CA., *Defense Technical Information Center* **1995**.
- [8] R. Rogoziński, InTechOpen **2015**, DOI: 10.5772/60641
- [9] J. R. Hensler (Bausch and Lomb Inc), *US3873408A*, **1975**.
- [10] R. H. Doremus, *J. Phys. Chem.* **1964**, 68, 2212–2218 (1964).
- [11] S. Ohmi et al., *Appl. Opt.* **1988**, 27, 496–499.
- [12] J.-L. Adam, X. Zhang, Chalcogenide Glasses: Preparation, Properties and Applications, Woodhead Publishing, **2014**.
- [13] L. Calvez et al., *Appl. Phys. A* **2007**, 89, 183–188.
- [14] A. Bornstein, T. Tsalach, E. Elyasaf, Y. Atiya, in *Proc SPIE 0819G* **1987**, *Infrared Technology XIII*, 150–157.
- [15] D. Gibson et al., in Proc SPIE 9451 **2015**, *Infrared Technology and Applications XLI*, 94511P.
- [16] D. Gibson et al., in Proc SPIE 9070 **2014**, *Infrared Technology and Applications XL*, 90702I.
- [17] D. Gibson et al., in Proc. SPIE 10181 **2017**, Adv. Opt. Def. Appl. UV LWIR II, 101810B.
- [18] D. Gibson, S. Bayya, J. Sanghera. *Class. Opt.* **2014**, OSA Technical Digest, IW2A.1
- [19] A. Lepicard et al., *Sci. Rep.* **2018**, 8, 7388
- [20] S. Novak et al., *ACS Appl. Mater. Interfaces* **2017**, 9, 26990–26995.
- [21] C. Baleine, T. Mayer, J. Musgraves, K. Richardson, P. Wachtel, *93404446*, **2016**.
- [22] L. Siskin et al., *Opt. Mater. Express* **2017**, 7, 3077–3092.
- [23] M. Kang et al., *Opt. Mater. Express* **2018**, 8, 2722–2733.
- [24] XH. Zhang et al., *J. Non-Cryst. Solids* **2004**, 337, 130–135.
- [25] L. Calvez, HL Ma, J. Lucas, & XH Zhang, *Adv. Mater* **2007**, 19, 129–132.
- [26] K. Hübner, *Phys. Status Solidi A*, **1977**, 40, 487–495.
- [27] A. Yadav et al. *Phys. Chem. Glas. - Eur. J. Glass Sci. Technol. Part B*, **2017**, 58, 115–126.
- [28] A. Yadav et al., *Int. J. Appl. Glass Sci.*, **2019**, 10, 27–40.
- [29] L. Siskin et al., *Adv. Func. Mater.* **2019**, DOI: 10.1002/adfm.201902217
- [30] M. Rozé, et al., *J. Am. Ceram. Soc.*, **2008**, 91, 3566–3570.
- [31] D. Lübbers, & V. Leute, *J. Solid State Chem.*, **1982**, 43, 339–345.
- [32] A. Grzechnik, S. Stølen, E. Bakken, T. Grande & M. Mezouar, *J. Solid State Chem.*, **2000**, 150, 121–127.
- [33] Zemax, Leading Optical Product Design Software for Engineering Teams, <https://www.zemax.com/>

This paper reports the first fabrication of a radial gradient refractive index lens for the midwave and longwave infrared. This fabrication is achieved by using spatially controlled crystallization of chalcogenide glass in an annular furnace. A non-destructive way to characterize such lenses is also introduced.

Enora Lavanant^{1,2}, Laurent Calvez^{1*}, François Chevire¹, Mathieu Rozé^{2*}, Thomas Hingant², Raphaël Proux², Yann Guimond², Xiang-Hua Zhang¹

Keyword: GRIN, Chalcogenide glass-ceramics, Infrared



Accepted Manuscript